Synthesis of *syn*- and *anti*-1-Amino-3-[18F]fluoromethyl-cyclobutane-1-carboxylic Acid (FMACBC), Potential PET Ligands for Tumor Detection

Laurent Martarello,[†] Jonathan McConathy,[†] Vernon M. Camp,[†] Eugene J. Malveaux,[†] Nicholas E. Simpson,[‡] Chiab P. Simpson,[‡] Jeffrey J. Olson,[§] Geoffrey D. Bowers,[§] and Mark M. Goodman*,[†]

Emory Center for Positron Emission Tomography, Department of Radiology, and Department of Neurosurgery, Emory University, 1364 Clifton Road, Northeast, Atlanta, Georgia 30322

syn- and *anti*-1-Amino-3-[18F]fluoromethyl-cyclobutane-1-carboxylic acid (FMACBC, **16** and **17**), analogues of *anti*-1-amino-3-[18F]fluorocyclobutyl-1-carboxylic acid (FACBC), were prepared to evaluate the contributions of C-3 substitution and configuration on the uptake of these radiolabeled amino acids in a rodent model of brain tumors. Radiofluorinated targets [18F]**16** and [18F]**17** were prepared by no-carrier-added radiofluorination from their corresponding methanesulfonyl esters **12** and **13**, respectively, with decay-corrected radiochemical yields of 30% for [18F]**16** and 20% for [18F]**17**. In amino acid transport assays performed in vitro using 9L gliosarcoma cells, both [18F]**16** and [18F]**17** were substrates for L type amino acid transport, while [18F]**17** but not [18F]**16** was a substrate for A type transport. Biodistribution studies in normal Fischer rats with [18F]**16** and [18F]**17** showed high uptake of radioactivity (>2.0% dose/ g) in the pancreas while other tissues studied, including liver, heart, lung, kidney, blood, muscle, and testis, showed relatively low uptake of radioactivity (<1.0% dose/g). In rats implanted intracranially with 9L gliosarcoma cells, the retention of radioactivity in tumor tissue was high at 5, 60, and 120 min after intravenous injection of [18F]**16** and [18F]**17** while the uptake of radioactivity in brain tissue contralateral to the tumor remained low (<0.3% dose/g). Ratios of tumor uptake to normal brain uptake for [18F]**16** were 7.5:1, 7:1, and 5:1 at 5, 60, and 120 min, respectively, while for [18F]**17** the ratios were 7.5:1, 9:1, and 9:1 at the same time points. This work demonstrates that like *anti*-[18F]FACBC, [18F]**16** and [18F]**17** are excellent candidates for imaging brain tumors.

Introduction

Positron emission tomography (PET) offers the highest spatial and temporal resolution of all nuclear medicine imaging modalities and allows quantitation of tracer concentrations in tissues.[1] PET has been extensively used in the past 25 years for functional characterization of tumors. 2-[18F]Fluorodeoxyglucose (FDG) has been the most widely used PET agent for detecting brain and systemic tumors, and it is reported that the magnitude of its uptake corresponds to tumor grade.[2−5] Although [18F]FDG is an effective tumor-imaging agent, [18F]FDG/PET imaging of brain tumors has several shortcomings.[6−11] First, the interpretation of [18F]FDG images of solid tumors is often complicated by high uptake due to nonneoplastic processes such as cerebral ischemia and inflammation. Second, brain tumors may be difficult to detect because of significant [18F]FDG uptake in adjacent normal brain tissue, which results in relatively low tumor to normal brain ratios. Thus, development of new PET radiopharmaceuticals to complement [18F]FDG remains an active field of research.[12]

A variety of amino acids containing the positron-emitting isotopes 11C and 18F have been prepared and evaluated for potential use in clinical oncology. These amino acids can be subdivided into two major categories. The first category is represented by radiolabeled naturally occurring amino acids such as [11C]valine, L-[11C]-leucine, L-[11C]methionine (Met), and L-[1-11C]tyrosine, and structurally similar analogues such as 2-[18F]fluoro-L-tyrosine and 4-[18F]fluoro-L-phenylalanine.[13−22] The movement of these amino acids across tumor cell membranes occurs predominantly through carrier-mediated transport by the sodium-independent L type amino acid transport system. The increased uptake and prolonged retention of these radiolabeled amino acids in tumors relative to normal tissue are due to significant and rapid regional incorporation into proteins as well as participation in other intracellular metabolic pathways.[23] Of these radiolabeled amino acids, [11C]Met has been the most extensively used in humans to detect tumors.[23−28] Although [11C]Met has proven useful in detecting brain and systemic tumors, it is susceptible to in vivo metabolism through multiple pathways that give rise to numerous radiolabeled metabolites.[29,30] Thus, kinetic analysis with the necessary accuracy for reliable measurement of tumor metabolic activity is difficult. It is also unclear as to whether radiolabeled amino acids that participate in protein synthesis are the best markers for grading tumors. Some studies of the kinetics of amino acid uptake in human cancer patients suggest that amino acid transport provides a more

* To whom correspondence should be addressed. Tel.: (404)727-9366. Fax: (404)727-3488. E-mail: mgoodma@emory.edu.
† Emory Center for Positron Emission Tomography.
‡ Department of Radiology.
§ Department of Neurosurgery.

Scheme 1. Synthesis of the Hydantoins **4** and **5**
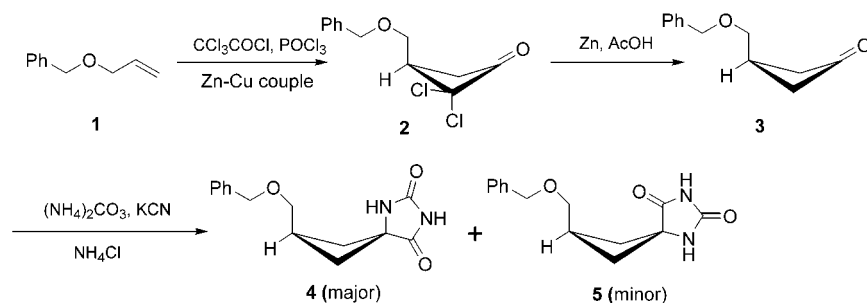
sensitive measurement of tumor cell proliferation than protein synthesis.[20-23]

The second category of amino acids has some significant advantages over the natural amino acids and their analogues. These are nonnatural amino acids such as [¹¹C]α-aminoisobutyric acid (AIB), 1-aminocyclopentane-1-[¹¹C]carboxylic acid (ACPC), and 1-aminocyclobutane-1-[¹¹C]carboxylic acid (ACBC).[31-37] These nonnatural amino acids are not metabolized, which simplifies the kinetic analysis of their uptake. On the basis of the promising results obtained with these nonnatural amino acids in preclinical studies, recent efforts have focused on the development of new ¹⁸F-labeled nonnatural amino acids, including *anti*-1-amino-3-[¹⁸F]fluorocyclobutyl-1-carboxylic acid (FACBC), L-[¹⁸F]fluoro-α-methyl tyrosine (FMT), and *O*-(2-[¹⁸F]fluoroethyl)-L-tyrosine (FET).[38-43]

The use of ¹⁸F offers a number of advantages over ¹¹C as a PET radionuclide, primarily because of its longer half-life (110 min for ¹⁸F vs 20 min for ¹¹C). From a radiochemistry and radiopharmacy perspective, ¹⁸F-labeled amino acids allow substantially more time for radiochemical synthesis, purification, and quality control of doses for human administration. As demonstrated by the clinical success of [¹⁸F]FDG, ¹⁸F-labeled radiopharmaceuticals can be synthesized in quantities sufficient for the formulation of multiple doses from a single production and for remote distribution to locations without on-site cyclotron facilities.

Of the recently reported ¹⁸F-labeled nonnatural amino acids, only [¹⁸F]FACBC has structural features and biological behavior consistent with significant transport by an amino acid transporter system other than the L type system. A structurally related alicyclic nonnatural amino acid, [¹¹C]ACPC, is a substrate for both the A type and the L type amino acid transporter systems.[44] The A type amino acid transport system is energy-dependent and can achieve high intracellular concentrations of substrate, while the L type system is not concentrative.[45] Our recent paper demonstrated that at 60 min following i.v. administration, [¹⁸F]FACBC showed high tumor to brain ratios of 6.6:1 in rats implanted with intracranial 9L gliosarcoma cells and 6.0:1 in a patient with glioblastoma multiforme.[40] Both [¹⁸F]FMT and [¹⁸F]FET are analogues of L-tyrosine and are selective substrates for the L type transport system. In studies of humans with brain tumors, [¹⁸F]FET achieved tumor to normal brain ratios ranging from 2:1 to 3:1.[42,43]

In this paper, we report the synthesis and biological evaluation of two novel nonnatural amino acids, *syn*-and *anti*-1-amino-3-fluoromethyl-cyclobutane-1-carboxylic acid (FMACBC; compounds **16** and **17**). We have

developed a high-yield radiolabeling method for both compounds that provides [¹⁸F]**16** and [¹⁸F]**17** in high radiochemical purity in a two step radiolabeling procedure. The biological behavior of these new radiotracers was examined through in vitro uptake assays using 9L gliosarcoma cells as well as biodistribution studies in normal and tumor-bearing rats to evaluate the effect of a fluoromethyl group at the 3-position of ACBC on tumor uptake and retention. On the basis of their high tumor to brain ratios in tumor-bearing rats, these radiotracers are attractive candidates for tumor imaging using PET.

Results and Discussion

Chemistry. Our approach to the synthesis of the fluorinated amino acids *syn*-1-amino-3-fluoromethyl-cyclobutane-1-carboxylic acid (**16**) and *anti*-1-amino-3-fluoromethyl-cyclobutane-1-carboxylic acid (**17**) involved the preparation of the hydantoins **4** and **5**, respectively, in which the primary hydroxyl function was protected with a benzyl group. The synthesis of the hydantoins is shown in Scheme 1. 3-(Benzyloxymethyl)-2,2-dichloro-cyclobutanone (**2**) was prepared by cycloaddition of dichoroketene to allyl benzyl ether (**1**) as previously described.[46] Subsequent reduction of the dichloro compound **2** with zinc dust in glacial acetic acid gave 3-(benzyloxymethyl)cyclobutanone (**3**) in very good yield.[46]

Initial syntheses of the hydantoins **4** and **5** from the ketone **3** using potassium cyanide and ammonium carbonate in an ethanol−water (1:1) solution provided **4** and **5** in 30−50% yield in a 4:1 syn:anti ratio as assessed by ¹H nuclear magnetic resonance (NMR). The yield was improved in subsequent reactions by including ammonium chloride in the reaction mix. Treatment of **3** with ammonium chloride, ammonium carbonate, and potassium cyanide afforded a mixture of 3-(benzyloxymethyl)cyclobutane hydantoins **4** and **5** in 70% yield with no effect on the isomeric ratio. Under these reaction conditions, the major isomer **4** has the syn configuration; its structure was confirmed by an X-ray crystal structure analysis (Figure 1). The stereoisomers were separated by silica gel column chromatography. It is interesting to note that like the synthesis of the 3-(benzyloxy)-cyclobutane hydantoin intermediates in the preparation of FACBC, the formation of the benzyloxymethyl derivatives is also stereoselective and that in both cases the major isomer possesses the syn conformation.[39]

Following chromatographic purification, hydantoins **4** and **5** were converted to their corresponding amino acids by the synthetic pathway shown in Scheme 2. The hydrolysis of the hydantoins **4** and **5** was achieved by
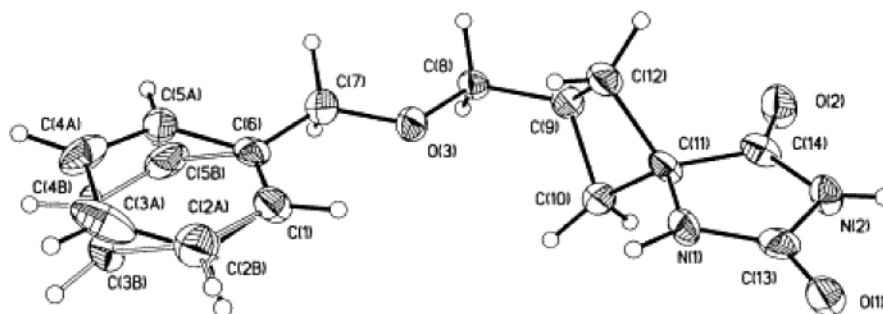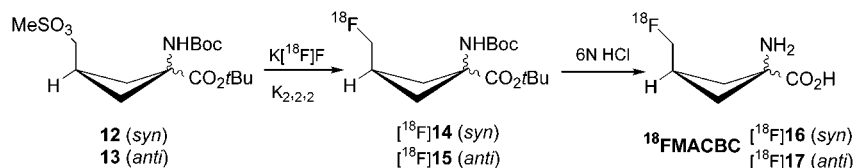
Figure 1. ORTEP view of compound **4** wherein about 52% of the molecules in the crystal had the "A" orientation of the phenyl ring, and the remaining 48%, the "B" conformation.

Scheme 2. Synthesis of *syn-* and *anti*-FMACBC (**16** and **17**)
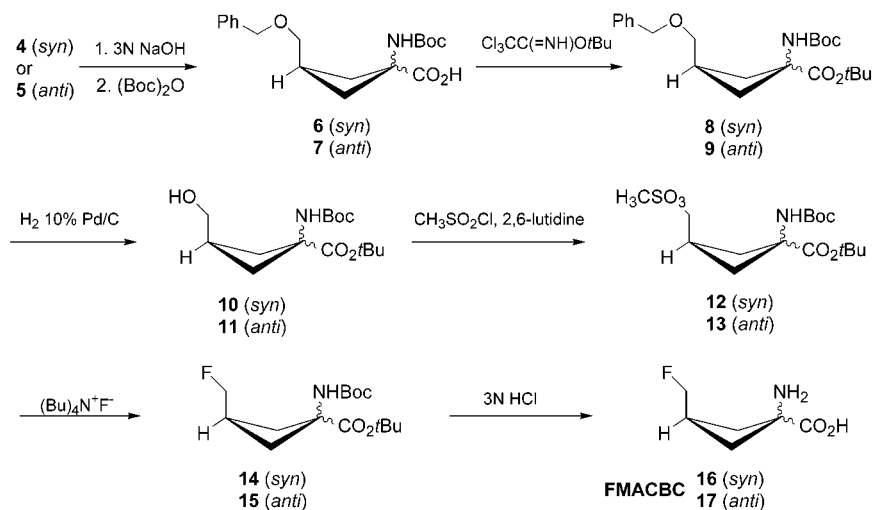
Scheme 3. Radiosynthesis of *syn-* and *anti*-[18F]FMACBC (**16** and **17**)

heating the substrate in a 3 N solution of sodium hydroxide in a sealed gas cylinder at 180 °C for 12 h. The amino acids were not isolated but were directly treated with di-*tert*-butyl dicarbonate to yield the *N*-Boc acids **6** and **7** in good yields (70 and 60% based upon **4** and **5**, respectively). In the next step, the protection of the carboxylic acid moiety was accomplished using *tert*-butyl-2,2,2-trichloroacetimidate to give the corresponding fully protected compounds **8** and **9** in 90% yield.[47] Hydrogenolysis of the benzyl ethers **8** and **9** was achieved using 10% palladium on charcoal and hydrogen to give alcohols **10** and **11** in quantitative yield.

Formation of the methanesulfonyl derivatives **12** and **13** was achieved using methanesulfonyl chloride and 2,6-lutidine in dichloromethane at room temperature. Treatment of the mesylates with tetrabutylammonium fluoride in tetrahydrofuran afforded a mixture of the fluorinated protected amino acids **14** and **15** and the hydrolyzed derivatives **10** and **11**. Finally, fluorinated intermediates **14** and **15** were deprotected using 3 N HCl at 60 °C for 30 min to afford *syn*-FMACBC (**16**) and *anti*-FMACBC (**17**), respectively.

Radiolabeling. *syn-* and *anti*-[18F]FMACBC were prepared from the mesylates **12** and **13** by no-carrier-added nucleophilic substitution with dried K[18F]F, potassium carbonate, and Kryptofix in acetonitrile (Scheme 3). The exchange between [18F]fluoride and the leaving group occurred in 10 min at 85 °C. Unreacted [18F]fluoride and radiolabeled polar byproducts were eliminated using solid phase extraction. We observed that under the same labeling conditions, the incorporation of [18F]fluorine was 1.5-fold higher in the case of the syn isomer [18F]**14** than the anti species [18F]**15**. Removal of protecting groups was achieved by acid hydrolysis using 6 N HCl at 85 °C for 10 min. The use of the *tert*-butyl ester group instead of the methyl ester to protect the carboxylic acid greatly reduced the temperature needed to ensure quantitative deprotection of the radiolabeled intermediate. For example, it took 10 min at 130 °C in a sealed vessel to achieve full deprotection of [18F]FACBC from the corresponding 1-[*N*-(*t*-butoxycarbonyl)amino]-3-[18F]fluoro-1-cyclobutane methyl ester.[40] Both amino acids were isolated by passing the acidic aqueous hydrosylate through an ion-retardation resin in series with an alumina N Sep-Pak and a C-18 Sep-Pak followed by elution with sterile water. The radiosyntheses were completed in 60 min following the end of bombardment (EOB) with overall

radiochemical decay-corrected yields of 30 (**16**, *n* = 3) and 20% (**17**, *n* = 3). Radio-thin-layer chromatography (TLC) showed >99% radiochemical purity. The eluted fractions were pH 6−7 and suitable for in vivo injection in rats.

The decay-corrected yields of both [^{18}F]**16** and [^{18}F]-**17** were comparable to those reported for other ^{18}F-labeled amino acids and are sufficient for multiple dose formulation from a single production. The published radiosynthesis of [^{18}F]FMT utilized nonradioactive fluorine carrier to achieve electrophilic substitution, which decreased the specific activity of the final product, and the desired product was obtained in approximately 10% decay-corrected yield.[41] Both [^{18}F]FET and [^{18}F]FACBC have been synthesized through no-carrier-added procedures, and these compounds were obtained in approximately 40 and 20% decay-corrected yields, respectively.[42,40]

In the radiosyntheses of both [^{18}F]**16** and [^{18}F]**17**, the maximum amount of unlabeled material in the final product arising from the precursors is about 3 mg in each case. On the basis of a 100 mCi yield at the end of synthesis (EOS), the minimum ratio of radiotracer to unlabeled material for both [^{18}F]**16** and [^{18}F]**17** is 1 mCi per 30 μg of unlabeled material. This amount of unlabeled material is comparable to the amount present in doses of [^{18}F]FDG.[48] However, the major byproducts of [^{18}F]FDG synthesis are glucose and mannose, which are not toxic. Although present in small amounts, the biological effects of the unlabeled material in [^{18}F]**16** and [^{18}F]**17** have not yet been evaluated. The potential toxicity of the unlabeled material present in the final dose must be evaluated prior to using [^{18}F]**16** and [^{18}F]-**17** in human studies.

Amino Acid Transport Assays. The biological transport of [^{18}F]**16** and [^{18}F]**17** was examined through uptake assays using cultured 9L gliosarcoma cells in the presence and absence of inhibitors of amino acid transport. *N*-methyl-α-aminoisobutyric acid (MeAIB) is a selective competitive inhibitor of the A type amino acid transport system. The unnatural amino acid 2-amino-bicyclo[2.2.1]heptane-2-carboxylic acid (BCH) is commonly used as an inhibitor of the sodium-independent L type transport system, although this compound also competitively inhibits amino acid uptake via the less abundant sodium-dependent B$^{0,+}$ and B^{0} transport systems.[45] The A and L type amino acid transport systems have been implicated in the in vivo uptake of radiolabeled amino acids used for tumor imaging.[23,44] A mixture of alanine, cysteine, and serine (ACS) was used to achieve a wide spectrum of amino acid transport inhibition to define the entry of [^{18}F]**16** and [^{18}F]**17** into 9L gliosarcoma cells by pathways other than amino acid transport. The amino acid uptake data expressed as percent uptake relative to the no inhibitor condition are shown in Figure 2.

In the absence of inhibitors, both [^{18}F]**16** and [^{18}F]**17** showed similar levels of uptake by 9L gliosarcoma cells, with accumulation of 2.9 and 2.3% of the initial dose per million cells after 30 min of incubation, respectively. In the presence of the ACS mixture, 97% of the cellular uptake of [^{18}F]**16** and 94% of [^{18}F]**17** was blocked relative to no inhibitor (*p* < 0.001 in both cases by one way analysis of variance (ANOVA)). This result indi-
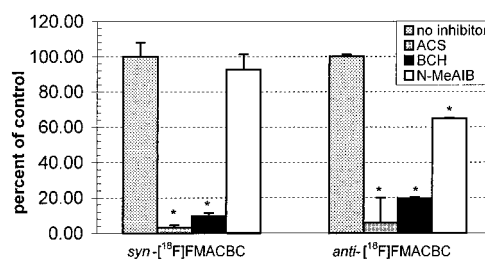
Figure 2. Inhibition of uptake of *syn*-[^{18}F]FMACBC (**16**) and *anti*-[^{18}F]FMACBC (**17**) by ACS, BCH, and *N*-MeAlB in 9L gliosarcoma cells. Values are expressed as percent of control uptake (no inhibitor). Uptake was determined after 30 min incubations and normalized for dose and number of cells. *p*-Values represent comparisons of uptake under each condition (one way ANOVA). * = *p* < 0.001 vs no inhibitor. Bars indicate standard deviation.

Table 1. Biodistribution of Radioactivity in Tissues of Fischer Rats Following Intravenous Administration of *syn*-[^{18}F]FMACBC (**16**)[a]

tissue	5 min	30 min	60 min	120 min
blood	0.53 ± 0.04	0.33 ± 0.04	0.32 ± 0.03	0.30 ± 0.03
heart	0.63 ± 0.03	0.67 ± 0.14	0.64 ± 0.08	0.60 ± 0.09
lung	0.75 ± 0.07	0.46 ± 0.01	0.46 ± 0.04	0.42 ± 0.05
liver	0.66 ± 0.06	0.37 ± 0.05	0.40 ± 0.02	0.52 ± 0.14
spleen	1.04 ± 0.11	0.58 ± 0.13	0.54 ± 0.05	0.54 ± 0.16
pancreas	4.43 ± 0.79	4.86 ± 1.10	3.13 ± 0.21	3.88 ± 0.64
kidney	0.57 ± 0.08	0.42 ± 0.08	0.45 ± 0.04	0.46 ± 0.08
bone	0.70 ± 0.10	0.32 ± 0.02	0.31 ± 0.01	0.32 ± 0.04
muscle	0.46 ± 0.05	0.58 ± 0.06	0.61 ± 0.01	0.60 ± 0.05
testis	0.32 ± 0.02	0.29 ± 0.07	0.23 ± 0.01	0.22 ± 0.02
brain	0.26 ± 0.02	0.24 ± 0.04	0.22 ± 0.01	0.21 ± 0.01

[a] Values are reported as mean percent dose per gram ± standard deviation; *n* = 4 at each time point.

cates that the vast majority of entry of these compounds into 9L tumor cells in vitro occurred via amino acid transport rather than a passive process. The uptake of [^{18}F]**16** and [^{18}F]**17** was significantly inhibited by BCH, with 90 and 80% inhibition relative to no inhibitor, respectively (*p* < 0.001 by one way ANOVA). In the presence of MeAIB, the uptake of [^{18}F]**16** was 93% of control uptake, and this reduction was not statistically different from the no inhibitor condition. In contrast, the uptake of [^{18}F]**17** was reduced by 35% relative to no inhibitor in the presence of MeAIB (*p* < 0.001 by one way ANOVA). The inhibition of uptake of [^{18}F]**17** by BCH was significantly greater than the inhibition by MeAIB (*p* < 0.001 by one way ANOVA).

These inhibition studies indicate that [^{18}F]**16** and [^{18}F]**17** enter 9L gliosarcoma cells through amino acid transport. Although BCH is not completely selective for the L type amino acid transport system, the large magnitude of uptake inhibition of [^{18}F]**16** and [^{18}F]**17** in the presence of BCH strongly suggests that these compounds are predominantly L type substrates. The inhibition of uptake of [^{18}F]**17** but not [^{18}F]**16** by MeAIB indicates that the configuration at the C-3 position influences amino acid transporter specificity and that [^{18}F]**17** entered 9L cells in part through A type transport.

Biodistribution in Normal Rats. Compounds [^{18}F]-**16** and [^{18}F]**17** showed similar biological profiles in normal rats as shown in Tables 1 and 2. For both [^{18}F]-**16** and [^{18}F]**17**, minimal defluorination was observed in vivo as measured by the low level of radioactivity in bone. The pancreas displayed the highest uptake of

Table 2. Biodistribution of Radioactivity in Tissues of Fischer Rats Following Intravenous Administration of *anti*-[18F]FMACBC (**17**)[a]

tissue	5 min	30 min	60 min	120 min
blood	0.57 ± 0.03	0.39 ± 0.06	0.33 ± 0.01	0.31 ± 0.02
heart	0.62 ± 0.09	0.68 ± 0.02	0.63 ± 0.12	0.55 ± 0.01
lung	0.91 ± 0.13	0.42 ± 0.01	0.41 ± 0.04	0.44 ± 0.05
liver	0.81 ± 0.06	0.41 ± 0.01	0.47 ± 0.02	0.48 ± 0.02
spleen	1.03 ± 0.11	0.63 ± 0.06	0.48 ± 0.04	0.47 ± 0.06
pancreas	2.56 ± 0.66	4.13 ± 0.81	3.83 ± 0.41	4.09 ± 0.23
kidney	0.76 ± 0.11	0.67 ± 0.05	0.66 ± 0.05	0.64 ± 0.08
bone	0.52 ± 0.04	0.31 ± 0.03	0.29 ± 0.03	0.29 ± 0.03
muscle	0.46 ± 0.05	0.57 ± 0.05	0.61 ± 0.03	0.61 ± 0.01
testis	0.24 ± 0.01	0.25 ± 0.02	0.24 ± 0.01	0.23 ± 0.01
brain	0.18 ± 0.01	0.24 ± 0.01	0.25 ± 0.03	0.25 ± 0.02

[a] Values are reported as mean percent dose per gram ± standard deviation; $n = 4$ at each time point.

radioactivity. The pancreatic uptake for [18F]**16** and [18F]-**17** was 4.43% of the injected dose per gram (ID/g) and 2.56% ID/g at 5 min, respectively. The uptake of radioactivity for [18F]**16** and [18F]**17** in the pancreas showed a peak at 30 min (4.86 and 4.13% ID/g, respectively) and remained high at 60 and 120 min. The other tissues studied, including liver, heart, lung, kidney, blood, muscle, and testis, showed relatively low uptake of radioactivity at 5 min (0.24−1.04% ID/g), which decreased over the course of the study except for the muscle and the heart where the retention of radioactivity remained almost constant. At 5 min, the brain showed low uptake of radioactivity for [18F]**16** and [18F]-**17**, with 0.26 and 0.18% ID/g, respectively. At 60 and 120 min, the brain retention remained low and constant when compared to the value at 30 min.

The distribution profiles of [18F]**16** and [18F]**17** in normal rats were very similar to previous results obtained with [18F]FACBC. As with [18F]**16** and [18F]-**17**, the highest levels of uptake were observed in the pancreas for [18F]FACBC (3.4% ID/g at 60 min). Most other tissues examined such as the heart, lung, kidney, muscle, and testis were relatively low after injection of [18F]FACBC (<0.6% ID/g at 60 min), although the uptake in the liver was 1.7% ID/g with [18F]FACBC at 60 min, which was approximately 4-fold higher than the uptake observed with [18F]**16** and [18F]**17**.[40] The presence of a fluoromethyl group at the C-3 position did not greatly alter these compounds' biological properties as compared to [18F]FACBC, and the component of A type transport observed for [18F]**17** in amino acid uptake assays did not dramatically alter the in vivo distribution profile relative to [18F]**16**.

Biodistribution in Tumor-Bearing Rats. The distributions of [18F]**16** and [18F]**17** at 5, 60, and 120 min after tail vein injection of these compounds in rats bearing intracranial 9L gliosarcoma implants are shown in Tables 3 and 4. With the exception of the pancreas, which showed a lower uptake of activity in tumor-bearing rats than in normal rats, the distribution of radioactivity of [18F]**16** and [18F]**17** in the organs of the tumor implanted rats showed a similar profile to that observed in normal rodents. The peak of activity in the pancreas for [18F]**16** and [18F]**17** was 3.19 and 3.26% ID/g, respectively, at 5 min. Unlike in normal rats where the uptake of activity of [18F]**16** and [18F]**17** in the pancreas remained relatively constant through 120 min, the activity after [18F]**16** and [18F]**17** injection in the

Table 3. Biodistribution of Radioactivity in Tissues of Tumor-Bearing Fischer Rats Following Intravenous Adminstration of *syn*-[18F]FMACBC (**16**)[a]

tissue	5 min	60 min	120 min
blood	0.44 ± 0.09	0.27 ± 0.02	0.24 ± 0.01
heart	0.52 ± 0.06	0.44 ± 0.06	0.33 ± 0.03
lung	0.57 ± 0.10	0.31 ± 0.04	0.26 ± 0.04
liver	0.64 ± 0.16	0.33 ± 0.07	0.25 ± 0.01
spleen	0.68 ± 0.06	0.41 ± 0.10	0.37 ± 0.07
pancreas	3.19 ± 0.74	2.08 ± 0.33	2.19 ± 0.44
kidney	0.59 ± 0.13	0.42 ± 0.01	0.34 ± 0.01
bone	0.26 ± 0.05	0.12 ± 0.04	0.13 ± 0.06
muscle	0.57 ± 0.06	0.54 ± 0.08	0.31 ± 0.15
testis	0.19 ± 0.01	0.22 ± 0.02	0.19 ± 0.01
brain	0.16 ± 0.04*	0.23 ± 0.01**	0.27 ± 0.12***
tumor	1.16 ± 0.11*	1.59 ± 0.22**	1.41 ± 0.19***
tumor:brain ratio	7.5:1	7:1	5:1

[a] Values are reported as mean percent dose per gram ± standard deviation; $n = 3$ at 5 min, $n = 4$ at 60 min, and $n = 3$ at 120 min. p-Values were determined using two-sided t-test for pairwise comparisons; * = $p < 0.007$, ** = $p < 0.001$, and *** = $p < 0.002$.

Table 4. Biodistribution of Radioactivity in Tissues of Tumor-Bearing Fischer Rats Following Intravenous Adminstration of *anti*-[18F]FMACBC (**17**)[a]

tissue	5 min	60 min	120 min
blood	0.51 ± 0.09	0.33 ± 0.03	0.30 ± 0.03
heart	0.58 ± 0.05	0.63 ± 0.07	0.52 ± 0.05
lung	0.55 ± 0.11	0.38 ± 0.03	0.36 ± 0.05
liver	0.87 ± 0.10	0.42 ± 0.04	0.35 ± 0.03
spleen	0.81 ± 0.10	0.45 ± 0.02	0.41 ± 0.07
pancreas	3.26 ± 0.56	2.48 ± 0.24	2.17 ± 0.48
kidney	0.96 ± 0.18	0.88 ± 0.17	0.79 ± 0.08
bone	0.31 ± 0.07	0.19 ± 0.06	0.19 ± 0.05
muscle	0.57 ± 0.07	0.60 ± 0.06	0.53 ± 0.06
testis	0.23 ± 0.04	0.26 ± 0.02	0.23 ± 0.02
brain	0.17 ± 0.07*	0.28 ± 0.02**	0.28 ± 0.05***
tumor	1.28 ± 0.23*	2.50 ± 0.19**	2.50 ± 0.17***
tumor:brain ratio	7.5:1	9:1	9:1

[a] Values are reported as mean percent dose per gram ± standard deviation; $n = 4$ at 5 and 60 min and $n = 5$ at 120 min. p-Values were determined using two-sided t-test for pairwise comparisons; * = $p < 0.001$, ** = $p < 0.0001$, and *** = $p < 0.0001$.

tumor-bearing rats showed a pronounced washout of 35 and 24%, respectively, at 60 min and 31 and 33%, respectively, at 120 min as compared to the 5 min values. The initial levels of activity in the tumors after injection of [18F]**16** or [18F]**17** were 1.16 and 1.27% ID/g at 5 min, respectively, while the uptake values in normal brain tissue from the contralateral cerebral hemisphere at 5 min were 0.16 and 0.17% ID/g, respectively. The activity in the tumor for [18F]**16** and [18F]**17** exhibited an increase of 37 and 96% at 60 min and remained almost constant at 120 min. Thus, ratios of tumor uptake to normal brain uptake for [18F]**16** were 7.5:1, 7:1, and 5:1 at 5, 60, and 120 min, respectively, while for [18F]**17** the ratios were 7.5:1, 9:1, and 9:1 at the same time points (Figure 3).

The tumor uptake of [18F]**17** was significantly higher than the uptake of [18F]**16** at both 60 and 120 min ($p < 0.001$ at 60 min and $p < 0.0001$ at 120 min by two-sided t-tests). Although both [18F]**16** and [18F]**17** showed comparable levels of in vitro uptake by 9L cells in the absence of inhibitor, the component of A type transport observed for [18F]**17** may be responsible for the higher tumor uptake in vivo. A type transport is energy-
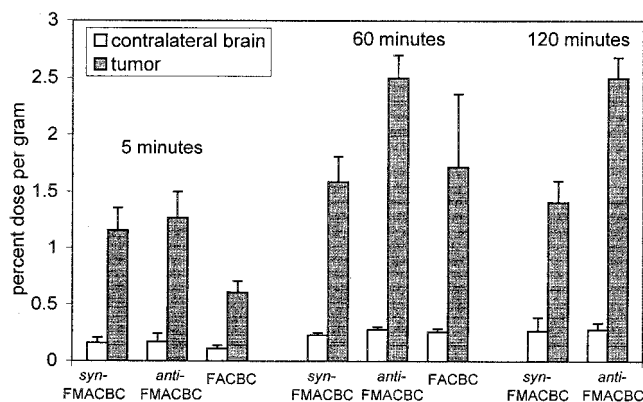
Figure 3. Activity in tumor and contralateral brain after injection of *syn*-[^{18}F]FMACBC (**16**), *anti*-[^{18}F]FMACBC (**17**), and [^{18}F]FACBC. Error bars represent standard deviation. Data for [^{18}F]FACBC are from ref 40.

dependent and can generate a concentration gradient, which could potentially lead to greater uptake, although establishing the role of A type transport in the in vivo behavior of [^{18}F]**17** will require further study. Because no data were collected between 5 and 60 min, it is possible that the maximum tumor to brain ratios were not observed. Dynamic PET imaging in animals with experimental tumors or in human cancer patients will be the most effective way to determine the in vivo kinetics of these compounds.

The tumor to brain ratios and the absolute value of the uptake of radioactivity achieved after injection of [^{18}F]**16** and [^{18}F]**17** are similar to those reported for [^{18}F]-FACBC in the same animal model.[40] At 5 and 60 min, the uptake of [^{18}F]FACBC in the tumor was 0.61 and 1.72% ID/g, respectively, resulting in tumor to brain ratios of 5.6 and 6.6 (see Figure 3). Similar tumor to brain ratios were observed in a study of a human patient with glioblastoma multiforme. When [^{18}F]FDG was evaluated in the same animal model, the uptake was 1.05% ID/g at 60 min in the tumor, and the tumor to brain ratio at this time was 0.8:1.[40] As in the normal tissues, the structural modification present in [^{18}F]**16** and [^{18}F]**17** did not greatly alter their uptake by 9L gliosarcoma tumors in comparison with [^{18}F]FACBC. However, the uptake of [^{18}F]**17** was about 50% higher than that of [^{18}F]**16** and [^{18}F]FACBC at 60 min, indicating that the C-3 position of the cyclobutyl ring does influence these compounds' biological behavior. All three of these ^{18}F-labeled amino acids showed higher uptake in tumor tissue and lower uptake in normal brain than [^{18}F]FDG.

In evaluating the biodistribution of novel radiolabeled amino acids for tumor imaging, it is important to consider the role of the blood–brain barrier (BBB). Charged compounds such as amino acids do not readily cross the normal BBB without biological transport, and high tumor to normal brain ratios could potentially be due to disruption of the BBB in the tumor vasculature. In the case of [^{18}F]**16** and [^{18}F]**17**, both the in vitro and the in vivo studies of their biological behavior demonstrate that these compounds are substrates for biological transport. Using skeletal muscle as a normal tissue for comparison avoids the potential confound of low uptake in normal brain due to an intact BBB. Tumor to muscle ratios also provide information about the potential

application of [^{18}F]**16** and [^{18}F]**17** to image systemic tumors with high uptake of these compounds. For [^{18}F]-**16**, the tumor to muscle ratio was 2.9:1 at 60 min and 4.5:1 at 120 min. In the case of [^{18}F]**17**, the tumor to muscle ratios were 4.1:1 at 60 min and 4.7:1 at 120 min. These results are similar to previous results obtained with [^{18}F]FACBC, which demonstrated a 4.1:1 tumor to muscle ratio at 60 min in the same rodent tumor model.[40] Comparison of the uptake of these amino acids relative to the uptake of [^{18}F]FDG provides further evidence for biological transport of [^{18}F]**16** and [^{18}F]**17** in vivo. Injection of [^{18}F]FDG led to a 5:1 tumor to muscle ratio at 60 min postinjection in this model with lower uptake in the tumor than observed with [^{18}F]**16** and [^{18}F]**17**. Uptake of activity after injection of [^{18}F]-FDG was 1.05% ID/g in tumor tissue at 60 min vs 1.59% ID/g for [^{18}F]**16** and 2.50% ID/g for [^{18}F]**17** at the same time point. If these radiolabeled amino acids were entering tumor tissue through diffusion alone, a lower absolute amount of uptake as compared to [^{18}F]FDG would be expected. In a study using a different rodent tumor model, injection of [^{18}F]FET in mice with xenotransplanted SW 707 colon carcinomas resulted in a tumor to muscle ratio of 2.7:1 at 60 min.[42] Taken together, these data support the conclusion that the tumor to brain ratios obtained with [^{18}F]**16** and [^{18}F]**17** are due to biological transport and do not simply reflect heterogeneous permeability of the BBB. The tumor to muscle ratios of uptake of radioactivity after injection of [^{18}F]**16** and [^{18}F]**17** are similar to those achieved with [^{18}F]FDG, suggesting that these radiolabeled amino acids might be useful for imaging systemic tumors.

Conclusions

The syn and anti isomers of FMACBC have been synthesized and radiolabeled with [^{18}F]fluorine in good yield (>20%) by a method very similar to that currently being used for [^{18}F]FDG. The radiosyntheses of [^{18}F]**16** and [^{18}F]**17** are readily adaptable for routine production using commercially available automated systems. Amino acid uptake assays using 9L gliosarcoma cells demonstrated that these compounds enter 9L cells in vitro primarily via L type amino acid transport, although [^{18}F]**17** undergoes some A type transport while [^{18}F]**16** does not. Biodistribution studies in rats showed that both [^{18}F]**16** and [^{18}F]**17** exhibited high uptake and prolonged retention in rat 9L gliosarcoma intracranial tumors and low uptake in normal brain tissue. These results were similar to those obtained with [^{18}F]FACBC in the same model. The anti configuration of the fluoromethyl group of [^{18}F]**17** led to an approximately 50–60% increase in tumor uptake of radioactivity over the syn isomer [^{18}F]**16** and [^{18}F]FACBC in this model. Both the in vitro cell uptake assays and the biodistribution studies demonstrate that the substituent and configuration at the C-3 position of ACBC influence the biological behavior of these compounds.

The very high tumor to brain ratios and in vivo stability to defluorination suggest that *syn*- and *anti*-FMACBC are excellent candidates for further evaluation for imaging tumors in humans. Studies in progress include in vitro uptake assays of both [^{18}F]**16** and [^{18}F]-**17** in cell lines derived from human tumors to establish the contributions of A type and L type amino acid

transport in the cellular uptake of these compounds in a variety of tumor types. An additional goal is the in vivo measurement of the regional distribution of [^{18}F]-**16** and [^{18}F]**17** following intravenous administration in severe combined immunodeficiency (SCID) mice implanted with the human tumor cells to determine their potential for imaging systemic tumors in humans.

Experimental Section

General Procedures. All animal experiments were carried out according to protocols by the Institutional University Animal Care Committee (IUCAC) and Radiation Safety Committees of Emory University. All chemicals and solvents were of analytical grade and were used without further purification. The [^{18}F]fluoride was produced at Emory University with a Siemens RDS 112 11 MeV negative-ion cyclotron by the ^{18}O (p,n) ^{18}F reaction using [^{18}O]H$_2$O (95%). TLC analyses were performed using either 0.25 mm thick layers of G PF-254 silica gel adsorbed on aluminum plates or 0.25 mm RP Chiralplates (Macherey-Nagel from Alltech Co., Deerfield, IL). Merck Kieselgel 60 was used for column chromatography. The proton NMR spectra were obtained with a 400 MHz Varian spectrometer. The chemical shift values are expressed in δ values (parts per million) relative to tetramethylsilane as an internal standard. Elemental analyses were obtained from Atlantic Microlab Inc., Norcross GA. Meltings points were measured with an Electrothermal 9100 apparatus (Electrothermal Eng. Ltd) and are uncorrected. Chromatograms of the radiolabeled compounds were analyzed with a Bioscan System 200 (Washington, DC).

syn- **and** ***anti-*2-[(Phenylmethoxy)methyl]-5,7-diazaspiro-[3.4]octane-6,8-dione (4 and 5).** To a stirring solution of ammonium carbonate (11.16 g, 116 mmol) and ammonium chloride (2.48 g, 46.3 mmol) in 75 mL of water was added a solution of the ketone **3** (2.2 g, 11.58 mmol) in 75 mL of ethanol. After 15 min, potassium cyanide (3.4 g, 52.3 mmol) was added and the reaction mixture was heated at 60 °C for 72 h. The solvent was removed by rotoevaporation. The resulting solid was stirred in water, and the crude product was collected by filtration. Chromatography of the crude solid on silica gel using CH$_2$Cl$_2$/MeOH (97:3) afforded 1.5 g (50%) of **4**, 0.47 g (16%) of **5**, and approximately 0.2 g of unresolved **4** and **5**.

***syn-*2-[(Benzyloxy)methyl]-5,7-diazaspiro[3.4]octane-6,8-dione (4).** mp 150−151 °C (CH$_2$Cl$_2$−MeOH). ^{1}H NMR (CDCl$_3$): δ 2.23 (dd, 2H, J = 13.2 and 6.8 Hz, CH$_2$), 2.52−2.61 (m, 1H, CH), 2.76 (dd, J = 12.2 and 9.4 Hz, CH$_2$), 3.48 (d, 2H, J = 4 Hz, OCH$_2$), 4.57 (s, 2H, Ph-CH$_2$−O), 6.15 (s, 1H, NH), 7.32−7.40 (m, 5H, phenyl), 7.97 (s, 1H, NH). Anal. (C$_{14}$H$_{16}$N$_2$O$_3$): C, H, N.

***anti-*2-[(Benzyloxy)methyl]-5,7-diazaspiro[3.4]octane-6,8-dione (5).** mp 173−174 °C (CH$_2$Cl$_2$−MeOH). ^{1}H NMR (CDCl$_3$): δ 2.35−2.43 (m, 2H, CH$_2$), 2.48−2.55 (m, 2H, CH$_2$), 2.62−2.72 (m, 1H, CH), 3.65 (d, 2H, J = 9.6 Hz, O−CH$_2$), 4.53 (s, 2H, Ph-CH$_2$−O), 6.37 (s, 1H, NH), 7.25−7.38 (m, 5H, phenyl), 8.15 (s, 1H, NH). Anal. (C$_{14}$H$_{16}$N$_2$O$_3$): C, H, N.

1-[*N-(tert*-Butoxycarbonyl)amino]-3-benzyloxymethyl-1-cyclobutane-1-carboxylic Acids (6 and 7). The appropriate isomerically pure hydantoin (0.3 g, 1.1 mmol) was hydrolyzed by heating with 13 mL of 3 N NaOH in a closed gas cylinder at 120 °C for 12 h. The clear yellow solution was neutralized to pH 6−7 with concentrated HCl and evaporated to dryness. The residue was extracted with 5 × 10 mL of hot methanol. Methanol aliquots were combined and evaporated to dryness. The resulting white solid was treated with di-*tert*-butyl dicarbonate (0.5 g, 2.3 mmol) in 10 mL of a mixture methanol/triethylamine (9:1) at room temperature for 12 h. The solvent was removed by rotoevaporation, and the crude product was chromatographed on silica gel using CH$_2$Cl$_2$/MeOH (95:5).

***syn-*1-[*N-(tert*-Butoxycarbonyl)amino]-3-benzyloxy-methyl-1-cyclobutane-1-carboxylic Acid (6).** Yield 0.31 g (84%); oil. ^{1}H NMR (CDCl$_3$): δ 1.43 (s, 9H, *t*-Bu), 2.05−2.18

(m, 2H, CH$_2$), 2.53−2.83 (m, 3H, CH$_2$ and CH), 3.48 (d, 2H, J = 4.8 Hz, OCH$_2$), 4.52 (s, 2H, Ph-CH$_2$−O), 5.15−5.26 (bs, 1H, NH), 7.27−7.36 (m, 5H, phenyl). Anal. (C$_{18}$H$_{25}$NO$_5$): C, H, N.

***anti-*1-[*N-(tert*-Butoxycarbonyl)amino]-3-benzyloxy-methyl-1-cyclobutane-1-carboxylic Acid (7).** Yield 0.28 g (76%); oil. ^{1}H NMR (CDCl$_3$): δ 1.45 (s, 9H, *t*-Bu), 2.50−2.53 (m, 4H, CH$_2$ ×2), 2.76−2.85 (m, 1H, CH), 3.54 (d, 2H, J = 5.6 Hz, OCH$_2$), 4.56 (s, 2H, PhCH$_2$−O), 5.39−5.44 (bs, 1H, NH), 7.27−7.36 (m, 5H, phenyl). Anal. (C$_{18}$H$_{25}$NO$_5$): C, H, N.

1-[*N-(tert*-Butoxycarbonyl)amino]-3-benzyloxymethyl-1-cyclobutane-1-carboxylic Acid *t*-Butyl Esters (8 and 9). A solution of *tert*-butyl 2,2,2,-trichloroacetimidate (0.68 g, 3.1 mmol) and the appropriate isomerically pure protected amino acid (0.335 g, 1 mmol) in 5 mL of dichloromethane was stirred 15 h at room temperature. The reaction mixture was concentrated to dryness and chromatographed on silica gel using CH$_2$-Cl$_2$/MeOH (98:2).

***syn-*1-[*N-(tert*-Butoxycarbonyl)amino]-3-benzyloxy-methyl-1-cyclobutane-1-carboxylic Acid *t*-Butyl Ester (8).** Yield 1.08 g (89%); mp 52.5 °C (CH$_2$Cl$_2$−MeOH). ^{1}H NMR (CDCl$_3$): δ 1.42 (s, 9H, NH*t*Bu), 1.48 (s, 9H, CO$_2$*t*Bu), 2.19−2.26 (m, 2H, CH$_2$), 2.56−2.64 (m, 3H, CH$_2$ and CH), 3.50 (bs, 2H, OCH$_2$), 4.51 (s, 2H, PhCH$_2$O), 5.2 (s, 1H, NH), 7.26−7.37 (m, 5H, phenyl). Anal. (C$_{22}$H$_{33}$NO$_5$): C, H, N.

***anti-*1-[*N-(tert*-Butoxycarbonyl)amino]-3-benzyloxy-methyl-1-cyclobutane-1-carboxylic Acid *t*-Butyl Ester (9).** Yield 1.12 g (92%); oil. ^{1}H NMR (CDCl$_3$): δ 1.43 (s, 18H, NH*t*-Bu and CO$_2$*t*Bu), 2.12−2.30 (m, 2H, CH$_2$), 2.34−2.42 (m, 2H, CH$_2$ and CH), 2.70−2.84 (m, 1H, CH), 3.50 (d, 2H, J = 7.2 Hz, OCH$_2$), 4.51 (s, 2H, PhCH$_2$O), 5.2 (s, 1H, NH), 7.26−7.36 (m, 5H, phenyl). Anal. (C$_{22}$H$_{33}$NO$_5$): C, H, N.

1-[*N-(tert*-Butoxycarbonyl)amino]-3-hydroxymethyl-1-cyclobutane-1-carboxylic Acid *t*-Butyl Esters (10 and 11). A suspension of the benzyl ether (120 mg, 0.31 mmol) and 10% Pd/C (20 mg) in 10 mL of methanol was stirred under a hydrogen atmosphere for 3 h. After it was filtered through a pad of Celite, the filtrate was concentrated to dryness under reduced pressure and purified via silica column chromatography using CH$_2$Cl$_2$/MeOH (98:2).

***syn-*1-[*N-(tert*-Butoxycarbonyl)amino]-3-hydroxy-methyl-1-cyclobutane-1-carboxylic Acid *t*-Butyl Ester (10).** Yield 92 mg (100%); oil. ^{1}H NMR (CDCl$_3$): δ 1.43 (s, 18H, NH*t*Bu and CO$_2$*t*Bu), 2.41−2.65 (m, 5H, CH$_2$−CH−CH$_2$), 3.66 (bs, 2H, CH$_2$OH), 5.49 (s, 1H, NH). Anal. (C$_{15}$H$_{27}$NO$_5$): C, H, N.

***anti-*1-[*N-(tert*-Butoxycarbonyl)amino]-3-hydroxy-methyl-1-cyclobutane-1-carboxylic Acid *t*-Butyl Ester (11).** Yield 90 mg (96%); mp 96 °C (CH$_2$Cl$_2$−MeOH). ^{1}H NMR (CDCl$_3$): δ 1.45 (s, 9H, NH*t*Bu), 1.50 (s, 9H, CO$_2$*t*Bu), 2.26 (bs, 2H, CH$_2$), 2.40−2.46 (m, 2H, CH$_2$), 2.62−2.74 (m, 1H, CH), 3.68 (d, 2H, J = 6.4 Hz, CH$_2$OH), 5.11 (s, 1H, NH). Anal. (C$_{15}$H$_{27}$NO$_5$): C, H, N.

1-[*N-(tert*-Butoxycarbonyl)amino]-3-mesyloxymethyl-1-cyclobutane-1-carboxylic Acid *t*-Butyl Esters (12 and 13). To a solution of the appropriate alcohol (90 mg, 0.3 mmol) and 2,6-lutidine (0.21 mL, 1.83 mmol) in 5 mL of dichloromethane at 0 °C under argon was added dropwise methanesulfonyl chloride (0.094 mL, 1.22 mmol). After 2 h at room temperature, water was added, and the organic phase was separated. The organic layer was successively washed with saturated NaHCO$_3$, cold 1 N HCl, and saturated NaCl. After the mixture was dried over sodium sulfate and the solvent was evaporated, the crude residue was purified by column chromatography using EtOAc/Hex (1:2).

***syn-*1-[*N-(tert*-Butoxycarbonyl)amino]-3-mesyloxy-methyl-1-cyclobutane-1-carboxylic Acid *t*-Butyl Ester (12).** Yield 90 mg (79%); mp 111 °C (EtOAc−Hex). ^{1}H NMR (CDCl$_3$): δ 1.43 (s, 9H, NH*t*Bu), 1.49 (s, 9H, CO$_2$*t*Bu), 2.38−2.47 (m, 2H, CH$_2$), 2.58−2.63 (m, 2H, CH$_2$), 2.70−2.80 (m, 1H, CH), 3.03 (s, 3H, SO$_2$CH$_3$), 4.30 (s, 2H, OCH$_2$), 5.34 (s, 1H, NH). Anal. (C$_{16}$H$_{29}$NO$_7$S): C, H, N.

***anti-*1-[*N-(tert*-Butoxycarbonyl)amino]-3-mesyloxy-methyl-1-cyclobutane-1-carboxylic Acid *t*-Butyl Ester (13).** Yield 95 mg (83%); mp 89−90 °C (EtOAc−Hex). ^{1}H NMR

(CDCl$_3$): δ 1.43 (s, 9H, NHtBu), 1.48 (s, 9H, CO$_2t$Bu), 2.38–2.48 (m, 4H, CH$_2$ ×2), 2.84–2.96 (m, 1H, CH), 3.01 (s, 3H, SO$_2$CH$_3$), 4.32 (d, 2H, J = 7.6 Hz, OCH$_2$), 5.21 (s, 1H, NH). Anal. (C$_{16}$H$_{29}$NO$_7$S): C, H, N.

1-[N-(*tert*-Butoxycarbonyl)amino]-3-fluoromethyl-1-cyclobutane-1-carboxylic Acid t-Butyl Esters (14 and 15). To a solution of the mesylate (37.9 mg, 0.1 mmol) in 5 mL of tetrahydrofuran under argon was added 1 N solution of tetrabutylammonium fluoride in tetrahydrofuran (0.12 mL, 0.12 mmol). The solution was stirred at room temperature for 4 days, with monitoring by TLC (EtOAc/Hex, 1:4) of the disappearance of the starting material. The solvent was then removed at reduced pressure, and the residue was purified by column chromatography using EtOAc–Hex (1:4).

***syn*-1-[N-(*tert*-Butoxycarbonyl)amino]-3-fluoromethyl-1-cyclobutane-1-carboxylic Acid t-Butyl Ester (14).** Yield 15 mg (50%); mp 70–71 °C (EtOAc–Hex). ^{1}H NMR (CDCl$_3$): δ 1.43 (s, 9H, NHtBu), 1.49 (s, 9H, CO$_2t$Bu), 2.21–2.30 (m, 2H, CH$_2$), 2.57–2.62 (m, 2H, CH$_2$), 2.62–2.75 (m, 1H, CH), 4.43 (d, 2H, J = 47 Hz, CH$_2$F), 5.22 (s, 1H, NH). Anal. (C$_{15}$H$_{26}$FNO$_4$): C, H, N.

***anti*-1-[N-(*tert*-Butoxycarbonyl)amino]-3-fluoromethyl-1-cyclobutane-1-carboxylic Acid t-Butyl Ester (15).** Yield 11 mg (35%); mp 85 °C (EtOAc–Hex). ^{1}H NMR (CDCl$_3$): δ 1.44 (s, 9H, NHtBu), 1.47 (s, 9H, CO$_2t$Bu), 2.22–2.36 (m, 2H, CH$_2$), 2.44–2.49 (m, 2H, CH$_2$), 2.78–2.94 (m, 1H, CH), 4.45 (dd, 2H, J = 47.4 and 6.4 Hz, CH$_2$F), 5.13 (s, 1H, NH). Anal. (C$_{15}$H$_{26}$FNO$_4$): C, H, N.

1-Amino-3-fluoromethyl-cyclobutane-1-carboxylic Acids (16 and 17). To a solution of protected amino acid (12 mg, 0.039 mmol) in 0.4 mL of methanol was added 1 mL of 3 N HCl. The reaction vessel was sealed and heated at 60 °C for 30 min, with monitoring by TLC (CH$_3$CN/MeOH/H$_2$O, 20:5:5) of the disappearance of the starting material. The solution was then loaded on an ion-retardation resin (AG 11A8 50–100 mesh) column in series with two alumina N Sep-Paks (wet) and a C18 Sep-Pak and eluted with water.

***syn*-1-Amino-3-fluoromethyl-cyclobutane-1-carboxylic Acid (16).** Yield 5 mg (87%); decomposition 250 °C. ^{1}H NMR (D$_2$O): 2.21–2.30 (m, 2H, CH$_2$), 2.57–2.62 (m, 2H, CH$_2$), 2.62–2.75 (m, 1H, CH), 4.43 (d, 2H, J = 47 Hz, CH$_2$F). Anal. (C$_6$H$_{10}$FNO$_2$): C, 48.97; H, 6.85; N, 9.52. Found: C, 49.85; H, 6.61; N, 9.81.

***anti*-1-Amino-3-fluoromethyl-cyclobutane-1-carboxylic Acid (17).** Yield 4.2 mg (73%); decomposition 250 °C. ^{1}H NMR (D$_2$O): 2.77–2.37 (m, 2H, CH$_2$), 2.53–2.59 (m, 2H, CH$_2$), 2.87–2.95 (m, 1H, CH), 4.55 (dd, 2H, J = 47 and 6.2 Hz, CH$_2$F). Anal. (C$_6$H$_{10}$FNO$_2$): C, H, N.

Radiolabeling. To a Wheaton 5 mL reaction vial containing 600 mCi of [^{18}F]fluoride in 350 mg of ^{18}O-water was added 1 mL of a solution consisting of 10 mg of Kryptofix, 1 mg of potassium carbonate, 0.05 mL of water, and 0.95 mL of acetonitrile. The solution was heated at 110 °C, and the solvent was evaporated with the aid of argon flow. The remaining moisture was removed by addition of 1 mL of dry acetonitrile to the vial followed by evaporation using argon flow. This process was repeated two more times to ensure dryness of the fluoride. A solution of the precursor (5 mg) in 1 mL of acetonitrile was introduced into the vial, and the no-carrier-added radiofluorination was performed at 85 °C for 10 min. The mixture was then diluted with 4 mL of ether, and unreacted [^{18}F]fluoride was removed by passage through a silica Sep-Pak. The Sep-Pak was rinsed with an additional 6 mL of ether, and the combined eluent was evaporated using argon flow. A 6 N solution of HCl (0.5 mL) was added to the dry residue, and the deprotection was achieved by heating the reaction vial for 10 min at 85 °C. The radiolabeled amino acid was isolated by passing the aqueous solution through an ion-retardation resin (AG 11A8 50–100 mesh) in series with two alumina Sep-Paks (wet) and a C18 Sep-Pak and using sterile water as the eluent. The synthesis was completed in 60 min after the EOB with an overall radiochemical yield of 116 mCi for [^{18}F]**16** (30% EOB, n = 3) and 80 mCi for [^{18}F]**17** (20% EOB, n = 3). Radio-TLC showed >99% radiochemical purity (Chiral-

plates, 20:5:5 acetonitrile/water/methanol, R_f = 0.67). The identity of the radiolabeled products [^{18}F]**16** and [^{18}F]**17** was confirmed by comparing the R_f of the radioactive product visualized with radiometric TLC with the R_f of the authentic ^{19}F compounds **16** and **17** visualized with ninhydrin stain.

X-ray Crystallography. Compound **4**, as a colorless plate with dimensions of $0.2 \times 0.12 \times 0.02$ mm^3, was used for data collection. The crystal was coated with Paratone N oil, suspended in a small fiber loop, and placed in a cooled nitrogen gas stream at 100 K on a Bruker D8 SMART APEX CCD sealed tube diffractometer with graphite monochromated Mo Kα (0.071 073 Å) radiation. A hemisphere of data was measured using a series of combinations of ϕ and Ω scans cell with 10 s frame exposures and 0.3° frame widths. Data collection, indexing, and initial cell refinements were all handled using SMART software. Frame integration and final cell refinements were carried out using SAINT software. The final cell parameters were determined from least-squares refinement on 8192 reflections. The SADABS program was used to carry out absorption corrections. The structure was solved using direct methods and difference Fourier techniques (SHELXTL, V5.10). Hydrogen atoms were placed in their expected chemical position using the HFIX command and were included in the final cycles of least squares with isotropic U_{ij} values related to the atoms ridden upon. The C–H distances were fixed at 0.93, 0.98 (methine), 0.97 (methylene), or 0.96 Å (methyl). All of the nonhydrogen atoms were refined anisotropically. Scattering factors and anomalous dispersion corrections are taken from the International Tables for X-ray Crystallography. Structure solution, refinement, graphics, and generation of publication materials were performed by using SHELXTL, V5.10 software.

Amino Acid Uptake Inhibition Assays. The 9L gliosarcoma cells were initially grown as monolayers in T-flasks containing Dulbecco's Modified Eagle's Medium (DMEM) under humidified incubator conditions (37 °C, 5% CO$_2$/95% air). The growth media was supplemented with 10% fetal calf serum and antibiotics (10 000 units/mL penicillin and 10 mg/mL streptomycin). The growth media was replaced three times per week, and the cells were passaged so that the cells would reach confluency in a week's time.

When the monolayers were confluent, cells were prepared for experimentation in the following manner. Growth media was removed from the T-flask, and the monolayer cells were exposed to 1 X trypsin:EDTA for ~1 min to weaken the protein attachments between the cells and the flask. The flask was then slapped, causing the cells to release. Supplemented media was added to inhibit the proteolytic action of the trypsin, and the cells were aspirated through an 18 Ga needle until they were monodisperse. A sample of the cells was counted under a microscope using a hemocytometer, and the live/dead fraction was estimated through trypan blue staining (>98% viability). The remainder of the cells was placed into a centrifuge tube and centrifuged at 75G for 5 min, and the supernatant was removed. The cells were then resuspended in amino acid/serum-free DMEM salts.

In this study, approximately 1×10^6 cells were exposed to either [^{18}F]**16** or [^{18}F]**17** (5 μCi) in 3 mL of amino acid free media $\pm$ transporter inhibitors (10 mM) for 30 min under incubator conditions in 12 mm × 75 mm glass vials. Each assay condition was performed in duplicate. After they were incubated, cells were twice centrifuged (75G for 5 min) and rinsed with ice-cold amino acid/serum-free DMEM salts to remove residual activity in the supernatant. The vials were placed in a Packard Cobra II Auto-Gamma counter, the raw counts were decay-corrected, and the activity per cell number was determined. The data from these studies (expressed as percent uptake relative to control) were graphed using Excel, with statistical comparisons between the groups analyzed using a one way ANOVA (GraphPad Prism software package).

Tumor Induction and Animal Preparation. All animal experiments were carried out under humane conditions and were approved by the Institutional Animal Use and Care Committee (IUCAC) at Emory University. Rat 9L gliosarcoma

cells were implanted into the brains of male Fischer rats as described previously.[40] Briefly, anesthetized rats placed in a stereotactic head holder were injected with a suspension of 4×10^4 rat 9L gliosarcoma cells (1×10^7 per mL) in a location 3 mm right of midline and 1 mm anterior to the bregma at a depth of 5 mm deep to the outer table. The injection was performed over the course of 2 min, and the needle was withdrawn over the course of 1 min to minimize the backflow of tumor cells. The burr hole and scalp incision were closed, and the animals were returned to their original colony after recovering from the procedure. Intracranial tumors developed that produced weight loss, apathy, and hunched posture in the tumor-bearing rats, and the animals were used at 17−19 days after implantation.

Rodent Biodistribution Studies. The tissue distribution of radioactivity was determined in 16 normal male Fischer 344 rats (200−250 g) after intravenous injection of ∼85 μCi of [^{18}F]-**16** or [^{18}F]**17** in 0.3 mL of sterile water. The animals were allowed food and water ad libitum before the experiment. Following anesthesia induced with an intramuscular injection of 0.1 mL/100 g of a 1:1 ketamine (500 mg/mL):xylazine (20 mg/mL) solution, the radiolabeled amino acid was injected into the rats via a tail vein catheter. Groups of four rats were sacrificed at 5, 30, 60, and 120 min after injection of the dose. The animals were dissected, and selected tissues were weighed and counted along with dose standards in a Packard Cobra II Auto-Gamma Counter. The raw counts were decay-corrected, and the counts normalized as the percent of total injected dose per gram of tissue (% ID/g).

The tissue distribution of radioactivity was also determined in tumor-bearing Fischer 344 rats following intravenous injection of ∼35 μCi of [^{18}F]**16** or [^{18}F]**17** in 0.3 mL of sterile water. The procedure was similar to that already described for normal rats with the following modifications. The tail vein injections were performed in awake animals using a RTV-190 rodent restraint device (Braintree Scientific) to avoid mortality accompanying anesthesia in the presence of an intracranial mass. Animals were sacrificed at 5, 60, or 120 min postinjection. The same tissues were assayed as in normal rats with the addition of the tumor tissue, and the corresponding region of brain contralateral to the tumor was excised and used for comparison. The uptake in the tumor and contralateral brain was compared via a two-tailed t-test for paired observations.

Supporting Information Available: X-ray crystallography data for **4**. This material is available free of charge via the Internet at http://pubs.acs.org.

References

(1) Goodman, M. M. Automated Synthesis of Radiotracers for Positron Emission Tomography Applications. In *Clinical Positron Emission Tomography (PET)*; Hubner, K. F., Buonocore, E., Collmann, J., Kabalka, G. W., Eds.; Mosby-Year Book, Inc.: St. Louis, MO, 1991; pp 110−122.

(2) DiChiro, G.; DeLaPaz, R. L.; Brooks, R. A.; et al. Glucose Utilization of Cerebral Gliomas Measured by [^{18}F]fluorodeoxyglucose and Positron Emission Tomography. *Neurology* **1982**, *32*, 1323−1329.

(3) Gupta, N. C.; Frick, M. P. Clinical applications of positron emission tomography in cancer. *CA Cancer J. Clin.* **1993**, *43*, 235−254.

(4) Conti, P. S. Introduction to imaging brain tumor metabolism with positron emission tomography. *Cancer Invest.* **1995**, *13*, 244−259.

(5) Conti, P. S.; Lilien, D. L.; Hawley, K.; Keppler, J.; Grafton, S. T.; Bading, J. R. PET and [^{18}F]FDG in oncology: a clinical update. *Nucl. Med. Biol.* **1996**, *23*, 717−735.

(6) Yamada, S.; Kubota, K.; Kubota, R.; Ido, T.; Tamahashi, N. High accumulation of fluorine-18-fluorodeoxyglucose in turpentine-induced inflammatory tissue. *J. Nucl. Med.* **1995**, *23*, 532−537.

(7) Fulhan, M. J.; Melisi, J. W.; Nishimiya, J.; Dwyer, A. J.; Dichiro, G. Neuroimaging of Juvenile Pilocytic Astrocytomas: An Enigma. *Radiology* **1993**, *189*, 221−225.

(8) Patronas, N. J.; Brooks, R. A.; DeLaPaz, R. L.; Smith, B. H.; et al. Glycolytic Rate (PET) and Contrast Enhancement (CT) in Human Cerebral Gliomas. *Am. J. Neuroradiol.* **1983**, *4*, 533−535.

(9) Fracavilla, T. L.; Miletich, R. S.; DiChiro, G.; Patronas, N. J.; et al. Positron Emission Tomography in the Detection of Malignant Degeneration of Low-Grade Gliomas. *Neurosurgery* **1989**, *24*, 1−5.

(10) Tyler, J. L.; Diksic, M.; Villemure, J. G.; et al. Metabolic and Hemodynamic Evaluation of Gliomas Using Positron Emission Tomography. *J. Nucl. Med.* **1987**, *28*, 1123−1133.

(11) Ginsberg, M. D.; Reivich, M.; Giandomenico, A.; Greenberg, J. Local Glucose Utilization in Acute Focal Cerebral Ischemia: Local Dysmetabolism and Diaschisis. *Neurology* **1997**, *27*, 1042−1048.

(12) Varagnolo, L.; Stokkel, M. P. M.; Mazzi, U.; Pauwels, E. K. ^{18}F-labeled radiopharmaceuticals for PET in oncology. *Nucl. Med. Biol.* **2000**, *27*, 103−112.

(13) Hubner, K. F.; Andrews, G. A.; Buonocore, E.; Hayes, R. L.; Washburn, L. C.; Collmann, I. R.; Gibbs, W. D. Carbon-11-labeled amino acids for the rectilinear and positron tomographic imaging of the human pancreas. *J. Nucl. Med.* **1979**, *20*, 507−513.

(14) Keen, R. E.; Barrio, J. R.; Huang, S. C.; Hawkins, R. A.; Phelps, M. E. In vivo cerebral protein synthesis rate with leucyl-transferase used as a precursor pool: determination of biochemical parameters to structure tracer kinetic models for positron emission tomography. *J. Cereb. Blood Flow Metab.* **1989**, *9*, 429−445.

(15) Leskin-Kallio, S.; Nagren, K.; Lehikoinen, P.; Ruotsalainen, U.; Teras, M.; Joensuu, H. Carbon-11-methionine and PET an effective method to image head and neck cancer. *J. Nucl. Med.* **1992**, *33*, 691−695.

(16) Inoue, T.; Kim, E.; Wong, C. L. Comparison of fluorine-18-fluorodeoxyglucose and carbon-11-methionine PET in detection of malignant tumors. *J. Nucl. Med.* **1996**, *37*, 1472−1476.

(17) Bolster, J. M.; Vaalburg, W.; Paans, A. M.; et al. Carbon-11 labeled tyrosine to study tumor metabolism by positron emission tomography (PET). *Eur. J. Nucl. Med.* **1986**, *12*, 321−324.

(18) De Wolde, H.; Pruim, J.; Mastik, M. F.; Koudstaal, J.; Molenaar, W. M. Proliferative activity in human brain tumors: comparison of histopathology and L-[1-^{11}C]tyrosine PET. *J. Nucl. Med.* **1997**, *38*, 1369−1374.

(19) Wienhard, K.; Herholz, K.; Coenen, H. H.; Rudolf, J.; Kling, P.; Stocklin, G.; Heiss, W. D. Increased amino acid transport into brain tumor measured by PET of L-(2-^{18}F)Fluorotyrosine. *J. Nucl. Med.* **1991**, *32*, 1338−1346.

(20) Mineura, K.; Kowada, M.; Shishido, F. Brain tumor imaging with synthesized ^{18}F-fluorophenlalanine and positron emission tomography. *Surg. Neurol.* **1989**, *31*, 468−469.

(21) Miura, S.; Murakami, M.; Kanno, I.; Iida, H.; Uemura, K. Phenylalanine transport in the living human brain by a dynamic PET of L-[2-^{18}F]-fluorophenylalanine. *Nippon Rinsho* **1992**, *50*, 1457−1460.

(22) Ito, H.; Hatazawa, J.; Murakami, M.; Miura, S.; et al. Aging effect on neutral amino acid transport at the blood-brain barrier measured with L-[2-^{18}F]-fluorophenylalanine and PET. *J. Nucl. Med.* **1995**, *36*, 1232−1237.

(23) Jager, P. L.; Vallburg, W.; Pruim, J.; et al. Radiolabeled amino acids: basic aspects and clinical applications in oncology. *J. Nucl. Med.* **2001**, *42*, 432−445.

(24) Lilja, A.; Bergstrom, K.; Hartvig, P. Dynamic study of supra-tentorial gliomas with L-methyl-^{11}C-methionine and positron emission tomography. *Am. J. Neuroradiol.* **1985**, *6*, 505−514.

(25) Derlon, J. M.; Bourdet, C.; Bustany, P.; et al. ^{11}C-L-methionine uptake in gliomas. *Neurosurgery* **1989**, *25*, 720−728.

(26) Kameyama, M.; Shirane, R.; Itoh, J.; et al. The accumulation of ^{11}C-methionine in cerebral glioma patients studied with PET. *Acta Neurochirurgica* **1990**, *104*, 8−12.

(27) Bergstrom, M.; Lundqvist, H.; Ericson, K.; et al. Comparison of the accumulation kinetics of L-methyl-^{11}C-methionine and D-methyl-^{11}C-methionine in brain tumors studied with positron emission tomography. *Acta Radiol.* **1987**, *28*, 225−229.

(28) Mosskin, M.; Von Holst, H.; Bergstrom, M.; et al. Positron emission tomography with ^{11}C-methionine and computed tomography of intracranial tumors compared with histopathologic examination of multiple biopsies. *Acta Radiol.* **1987**, *28*, 673−681.

(29) Hatazawa, J.; Ishiwata, K.; Itoh, M.; et al. Quantitative evaluation of L-methyl-C-11-methionine uptake in tumor using positron emission tomography. *J. Nucl. Med.* **1989**, *30*, 1809−1813.

(30) Ishiwata, K.; Hatazawa, J.; Kubota, K.; et al. Metabolic fate of L-methyl-^{11}C-methionine in human plasma. *Eur. J. Nucl. Med.* **1989**, *15*, 665−669.

(31) Schmall, B.; Conti, P. S.; Bigler, R. E.; et al. Imaging studies of patients with malignant fibrous histiocytoma using C-11-α-aminoisobutyric acid (AIB). *J. Nucl. Med.* **1982**, *12*, 22−26.

(32) Schmall, B.; Conti, P. S.; Bigler, R. E.; et al. Synthesis and quality assurance of C-11 α-aminoisobutyric acid (AIB), a potential radiotracer for imaging and amino acid transport studies in normal and malignant tissues. *Int. J. Nucl. Med. Biol.* **1984**, *3*, 209−214.

(33) Conti, P. S.; Sordillo, P. P.; Schmall, B.; Buena, R. S.; Bading, J. R.; Bigler, R. E.; Laughlin, J. S. Tumor imaging with carbon-11 labeled α-aminoisobutyric acid (AIB) in a patient with advanced malignant melanoma. *Eur. J. Nucl. Med.* **1986**, *12*, 353−356.

(34) Sordillo, P. P.; DiResta, G. R.; Fissekis, J.; et al. Tumor imaging with carbon-11 labeled α-aminoisobutyric acid (AIB) in patients with malignant melanoma. *Am. J. Physiol. Imaging* **1991**, *7*, 2−11.

(35) Hubner, K. F.; Krauss, S.; Washburn, L. C.; et al. Tumor detection with 1-aminocyclopentane and 1-amino-cyclobutane C-11-carboxylic acid using positron emission computerized tomography. *Clin. Nucl. Med.* **1981**, *6*, 249−252.

(36) Hubner, K. F.; Thie, J. A.; Smith, G. T.; Kabalka, G. W.; Keller, I. B.; Kliefoth, A. B.; Campbell, S. K.; Buonocore, E. Positron Emission Tomography (PET) with 1-Aminocyclobutane-1-[11C]-carboxylic Acid (1-[11C]-ACBC) for Detecting Recurrent Brain Tumors. *Clin. Positron Imaging* **1998**, *1*, 165.

(37) Conti, P. S.; Sordillo, P. P.; Sordillo, E. M.; Schmall, B. Tumor localization of the metabolically trapped radiolabeled substrates 2-deoxy-D-glucose and animocyclopentanecarboxylic acid in human melanoma heterotransplants. *Am. J. Clin. Oncol.* **1986**, *9*, 537−540.

(38) Goodman, M. M.; Shoup, T. M.; Cullom, S. J.; et al. Initial Evaluation of High Energy NaI−Based Coincidence Brain Imaging of Tumor Amino Acid Uptake and Striatal Dopamine Transporters with [F-18]FACBC and [F-18]FECNT. *J. Nucl. Med.* **1997**, *38*, 1−152.

(39) Shoup, T. M.; Goodman, M. M. Synthesis of [F-18]-1-amino-3-fluorocyclobutane-1-carboxylic acid (FACBC): a PET tracer for tumor delineation. *J. Labelled Compd. Radiopharm.* **1999**, *42*, 215−225.

(40) Shoup, T. M.; Olson, J.; Hoffman, J. M.; et al. Synthesis and evaluation of [18F]1-amino-fluorocyclobutane-1-carboxylic acid to image brain tumors. *J. Nucl. Med.* **1999**, *40*, 331−338.

(41) Inoue, T.; Tomiyoshi, K.; Higuichi, T.; et al. Biodistribution studies on L-[18F]fluoro-α-methyl tyrosine: a potential tumor imaging agent. *J. Nucl. Med.* **1998**, *39*, 663−667.

(42) Wester, H. J.; Herz, M.; Weber, W.; Heiss, P.; Schmidtke, R. S.; Schwaiger, M.; Stocklin, G. Synthesis and Radiopharmacology of O-(2-[18F]fluoroethyl)-L-tyrosine for Tumor Imaging. *J. Nucl. Med.* **1999**, *40*, 205−212.

(43) Weber, W. A.; Wester, H. J.; Grosu, A. L.; Herz, M.; Dzewas, B.; Feldman, H. J.; Molls, M.; Stocklin, G.; Schwaiger, M. O-(2-[18F]-Fluoroethyl)-1-tyrosine and 1-[methyl-11C]methionine uptake in brain tumors: initial results of a comparative study. *Eur. J. Nucl. Med.* **2000**, *27*, 542−549.

(44) Uehara, H.; Miyagawa, T.; Tjuvajev, J.; et al. Imaging experimental brain tumors and 1-aminocyclopentane carboxylic acid and alpha-aminoisobutyric acid: comparison to fluorodeoxyglucose and diethylenetriaminepentaacetic acid in morphologically defined tumor regions. *J. Cereb. Blood Flow Metab.* **1997**, *17*, 1239−1253.

(45) Palacín, M.; Estévez, R.; Bertran, J.; Zorzano, A. Molecular biology of mammalian plasma membrane amino acid transporters. *Physiol. Rev.* **1998**, *78*, 969−1054.

(46) Kaiwar, V.; Reese, C. B.; Gray, E. J.; Neidle, S. Synthesis of 9-[cis-3-(hydroxymethyl)cyclobutyl]adenine and -guanine. *J. Chem. Soc., Perkin Trans. 1* **1995**, 2281−2287.

(47) Thierry, J.; Yue, C.; Potier, P. 2-Phenyl isopropyl and *tert*-butyl trichloroacetimidates: useful reagents for ester preparation of *N*-protected amino acids under neutral conditions. *Tetrahedron Lett.* **1998**, *39*, 1557−1560.

(48) Alexoff, D. L.; Casati, R.; Fowler, J. S.; et al. Ion chromatographic analysis of high specific activity 18FDG preparations and detection of the chemical impurity 2-deoxy-2-chloro-D-glucose. *Int. J. Rad. Appl. Instrum. Part A* **1992**, *4*, 1313−22.